



University of  
New Haven

University of New Haven  
**Digital Commons @ New Haven**

---

Department of Forensic Science Publications

Forensic Science

---

9-19-2016

# Collecting Quality Infrared Spectra from Microscopic Samples of Suspicious Powders in a Sealed Cell

Brooke Weinger Kammrath

*University of New Haven, bkammrath@newhaven.edu*

Pauline E. Leary

*Smiths Detection, Inc.*

John A. Reffner

*CUNY John Jay College of Criminal Justice*

Follow this and additional works at: <http://digitalcommons.newhaven.edu/forensicscience-facpubs>



Part of the [Forensic Science and Technology Commons](#)

---

## Publisher Citation

Kammrath, B. W., Leary, P.E., & Reffner, J.A. (2016). Collecting Quality Infrared Spectra from Microscopic Samples of Suspicious Powders in a Sealed Cell. *Applied Spectroscopy*. doi: 10.1177/00037028166662860. epub ahead of print Sept 19, 2016.

## Comments

This is the authors' accepted manuscript of the article published in *Applied Spectroscopy*. The version of record can be found at <http://dx.doi.org/10.1177/0003702816666286>

# **Collecting Quality Infrared Spectra from Microscopic Samples of Suspicious Powders in a Sealed Cell**

Brooke W. Kammrath<sup>1</sup>, Pauline E. Leary<sup>2</sup> and John A. Reffner<sup>3</sup>

<sup>1</sup> Department of Forensic Science, University of New Haven, 300 Boston Post Rd, West Haven, CT 06516

<sup>2</sup> Smiths Detection, 2202 Lakeside Blvd, Edgewood, MD 21040

<sup>3</sup> Department of Sciences, John Jay College of Criminal Justice, 524 West 59<sup>th</sup> Street, New York, NY 10019

## **Abstract**

The infrared microspectroscopical analysis of samples within a sealed-cell containing barium fluoride is a critical need when identifying toxic agents or suspicious powders of unidentified composition. The dispersive nature of barium fluoride is well understood and experimental conditions can be easily adjusted during reflection-absorption measurements to account for differences in focus between the visible and infrared regions of the spectrum. In most instances, the ability to collect a viable spectrum is possible when using the sealed cell regardless of whether visible or infrared focus is optimized. However, when infrared focus is optimized, it is possible to collect useful data from even smaller samples. This is important when minimal sample is available for analysis, or the desire to minimize risk of sample exposure is important. While the use of barium fluoride introduces dispersion effects that are unavoidable, it is possible to adjust instrument settings when collecting infrared spectra in the absorption-reflection mode to compensate for dispersion and minimize impact on the quality of the sample spectrum.

## **Keywords**

Infrared Microspectroscopy, Sealed Cell, Dispersion, Barium Fluoride

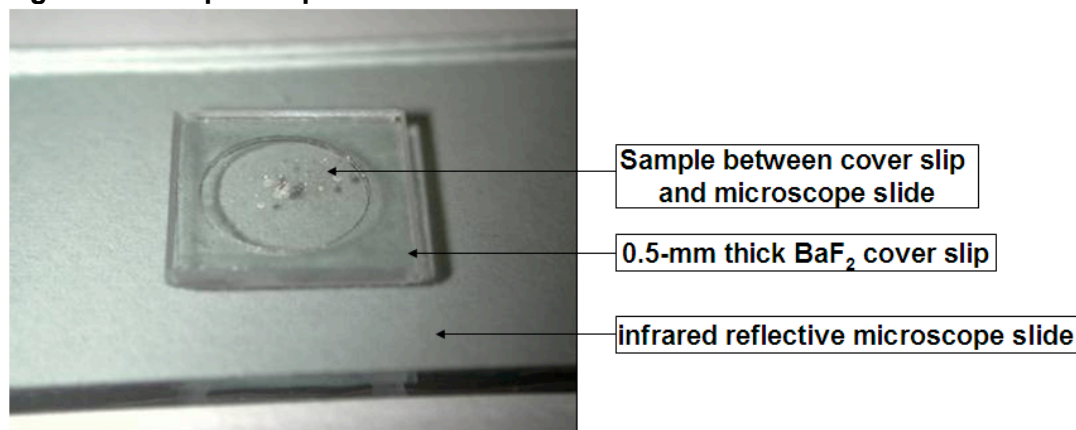
## **Introduction**

In response to the needs of the homeland-security and public-health-laboratory markets, sealed cells were developed to extend the application of the infrared microscope to the analysis of harmful agents or samples of unknown, unidentified or potentially toxic composition. Sealed cells enable the analyst to remain isolated and safe from the sample during preparation and analysis, and may be used effectively in the field to support the capabilities of mobile analytical laboratories. This is especially important in situations where unidentified chemical and biological threats pose an immediate danger to the public and must be safely and accurately identified at the scene.

The procedure for preparing a sample in a sealed cell involves transferring the sample to an infrared-reflective microscope slide within a glovebox. The sample is then encased using adhesive under a barium fluoride cover slip. The adhesive used is impermeable to both toxic agents and corrosive chemicals. The use of barium fluoride as the cover slip is appropriate because of its resistance to chemicals, insolubility in water, and transparency in both the visible and infrared regions of the spectrum. These properties make it possible to decontaminate the sealed cell after it is prepared so that a safe analysis may be performed. After decontamination, the preparation is removed from the glovebox and transferred to the stage of the infrared microscope for Fourier-transform infrared (FT-IR) microspectroscopical analysis in reflection-absorption mode. The all-reflecting objective (ARO) is used for this analysis, which is an objective that

enables the simultaneous collection of a visible image and the FT-IR spectra of a sample. An image of a sample prepared in a sealed cell is shown in Figure 1.

**Figure 1. Sample Prepared in a Sealed Cell.**



Preparation of the sample in the sealed cell makes it possible to safely and effectively perform FT-IR microspectroscopical analysis of toxic substances, but the properties of the sealed cell, specifically the refractive index and thickness of the barium fluoride cover slip, may impact spectral quality. A decrease in spectral quality may decrease the ability to perform an identification either by visual observation of the spectrum, or when performing electronic searches of spectra against spectral databases. It is, however, possible to adjust instrument settings to account for the factors that impact spectral quality to improve spectral quality and library-search results.

### Dispersion of Barium Fluoride

It is important to understand the interaction of light with barium fluoride in both the visible and infrared spectral regions in order to optimize infrared microspectroscopical analysis when a sealed cell is used. Infrared and visible radiation travel along the same path in air, but refract differently when entering and exiting barium fluoride. These refraction differences are shown in Figure 2 and are due to the dispersion of infrared and visible light in barium fluoride. Dispersion is the phenomenon in which a wave's velocity varies with its wavelength. Dispersion can be exploited for benefit, such as when used to separate white light by prisms; it can also be problematic such as when chromatic aberration in lenses challenge optimal visual observation. The infrared and visible dispersion curves for barium fluoride are shown in Figure 3, and were made using the dispersion formula:

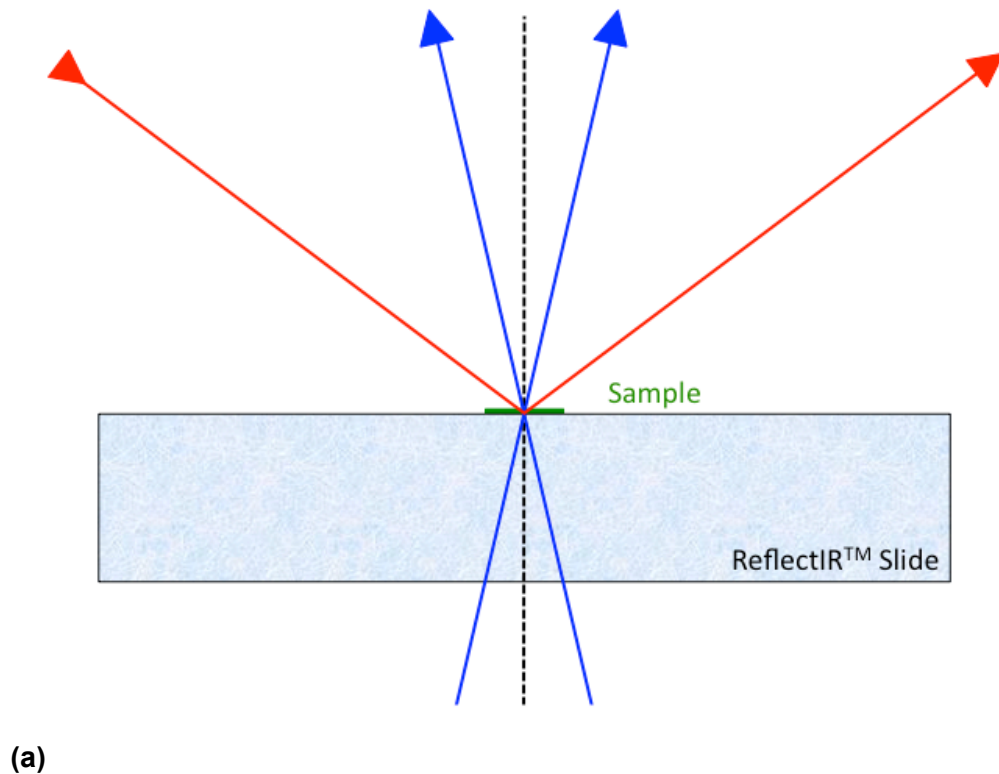
$$n^2 - 1 = C_1 \lambda^2 / (\lambda^2 - C_2^2) + C_3 \lambda^2 / (\lambda^2 - C_4^2) + C_5 \lambda^2 / (\lambda^2 - C_6^2) \quad (1)$$

where  $\lambda$  is the wavelength of light, and the dispersion constants of light through barium fluoride are  $C_1 = 0.643356$ ,  $C_2 = 0.057789$ ,  $C_3 = 0.506762$ ,  $C_4 = 0.10968$ ,  $C_5 = 3.8261$ , and  $C_6 = 46.3864$ .<sup>1</sup>

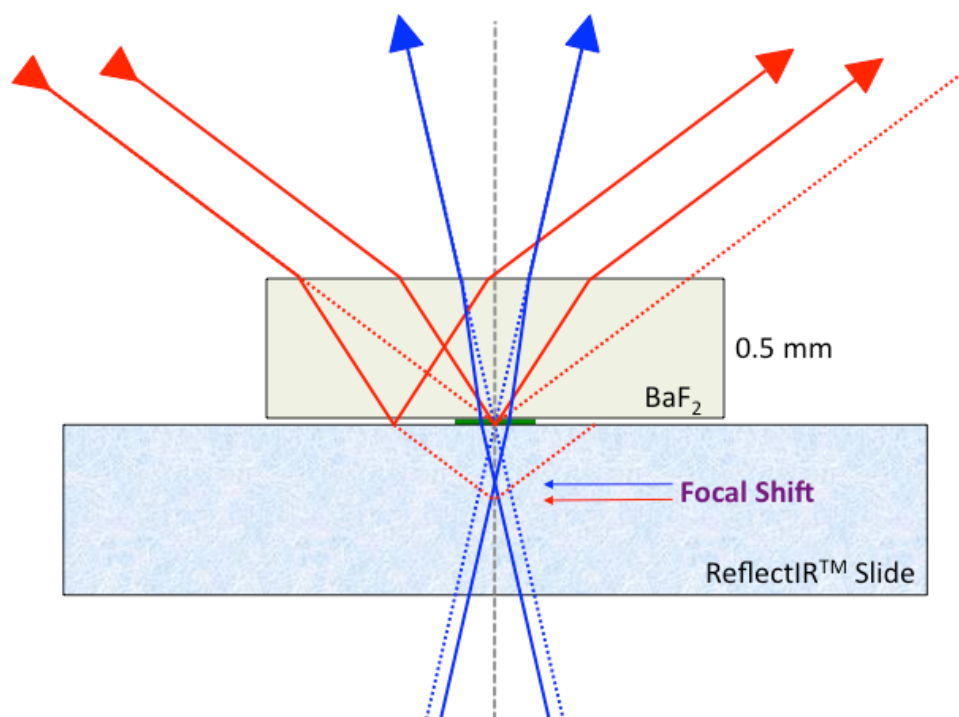
Wave velocity differences resulting from transmission of infrared and visible radiation through a sealed cell will adjust the plane of focus differently for the two different types of radiation. The degree of separation of the infrared and visible rays, called the focal shift, increases as barium fluoride thickness increases. Carr<sup>2</sup> and Wetzel<sup>3</sup> investigated the focal shift caused by the dispersion of barium fluoride

substrates. Infrared microspectrophotometers are designed so that the infrared and visible light detectors are parfocal in air, but the separation of rays in barium fluoride compromises this parfocality. This then requires that the system be aligned to either optimal focus for the visible ray or optimal focus for the infrared ray. It seems more typical for users to optimize for visual results rather than for infrared spectral quality. Experiments performed as described in this research were designed to determine whether the visible or infrared should be optimized when using the sealed-cell kit.

**Figure 2. Schematic of the Refraction of Visible and Infrared Radiation (Blue and Red Lines, Respectively) Through the Infrared Microscope Reflection-Absorption Objective, (a) With and (b) Without a Barium Fluoride Cover Slip.**

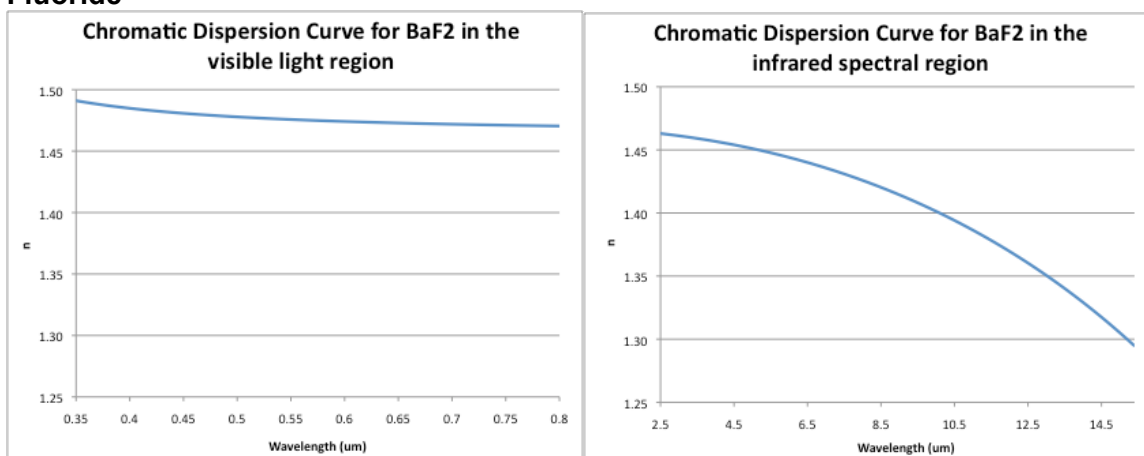






(b)

**Figure 3. Chromatic Dispersion of Visible and Infrared Radiation in Barium Fluoride**



Chan and Kazarian<sup>4,5</sup> developed a correction for the focal shift problem caused by the dispersion of different wavelengths of radiation in infrared imaging through an infrared window. Their research focused on improving the collection of infrared images of live cells in a liquid cell, and relies on the addition of a hemisphere to the surface of the liquid cell to prevent the refraction of the different wavelengths of radiation. This hemisphere is made of the same material as the liquid cell, which in their application is calcium fluoride. This could have potential for improving the collection of FT-IR spectra of samples in a sealed cell by removing the dispersion of visible and IR radiation.

However significant research on the curvature, interface and engineering of the hemisphere, as well as cost of manufacturing and field-testing would need to be performed prior to its implementation.

### Experiment Design

The goal of this study was to determine whether, when using a sealed cell with a barium fluoride cover slip, analysis in infrared focus or analysis in visible focus would generate better results. Better results were defined as the data set that generated the best hit quality index (HQI) when an infrared spectrum collected was compared with a library spectrum of the same compound. Both correlation and first-derivative-correlation algorithms were used during the comparisons.

The correlation algorithm of an unknown to a library entry is “effectively a normalized least squares dot product on the unknown”, where “both the unknown and the library data are centered about their respective means before the vector dot products are calculated”.<sup>6</sup> The advantage of centering the data is that it enables the HQI to be independent of the normalization of the spectra. This minimizes the effects on the HQI of a noisy baseline and sharp negative dips in the unknown spectrum due to the atmospheric interferences of water vapor and carbon dioxide peaks. The following equation is used to calculate the HQI:

$$HQI = 1 - \frac{(Lib_m \bullet Unkn_m)^2}{(Lib_m \bullet Lib_m)(Unkn_m \bullet Unkn_m)} \quad (2)$$

In equation 2, the library data ( $Lib_m$ ) and the unknown data ( $Unkn_m$ ) are defined as:

$$Lib_m = Lib - \frac{\sum_{i=f}^n Lib_i}{n} \quad (3)$$

$$Unkn_m = Unkn - \frac{\sum_{i=f}^n Unkn_i}{n} \quad (4)$$

The first derivative correlation algorithm is the same as the correlation algorithm, except prior to calculating the HQI, the first derivative of the library and known spectra are taken. The first derivative calculation is performed after mean centering. The first derivative calculation is done by subtracting previous points. The most common advantage of this is to help correct for bad baselines. Another advantage is with the analysis of broad peaks, as the derivative reveals the slope of the curve.<sup>6</sup>

The set of samples analyzed, sometimes referred to as the hoax-powder panel, are shown in Table 1.<sup>7</sup> These samples are commonly used as biological weapon hoaxes in order to mislead law enforcement and threaten public health. They are commonly analyzed using the sealed cell.

**Table 1. Samples Analyzed to Evaluate Optimal Procedure for Infrared Spectral Data Collection**

Hoax Powders Analyzed
Albumin
Baking Soda
Chalk
Dairy Creamer
Dipel
Dry Milk
Flour
Foot Powder
Kaolin
Non Dairy Creamer
Powdered Cleanser
Powdered Sugar
Spackling Powder
Talcum Powder
Yeast

### Library Preparation

For each sample, a few grains were transferred to an infrared-reflective slide and rolled to flatness using a stainless steel roller. Three spectra were collected in the reflection-absorption mode using the Smiths Detection IlluminatIR II with a 15-times ARO. The experimental conditions used were a 100- $\mu\text{m}$  by 100- $\mu\text{m}$  spot size, 4- $\text{cm}^{-1}$  spectral resolution, 64 background co-added scans and 64 sample co-added scans. The three spectra were averaged using Thermo GRAMS/AI software, and processed to eliminate the carbon dioxide peak (2400 – 2300  $\text{cm}^{-1}$ ). These spectra were then made into a searchable infrared library using Smiths Detection ChemID software.

### Focal Shift Measurement and Calculation

The magnitude of the focal shift was both experimentally measured and theoretically calculated. The focal shift was measured using a photoresist slide with a barium fluoride cover slip. The plane of optimum visual focus was established, and then the microscope stage was adjusted while simultaneously monitoring the interferogram signal until the maximum interferogram signal was achieved. Analysis was performed in triplicate by two scientists and equaled 91.5 +/- 0.5  $\mu\text{m}$ .

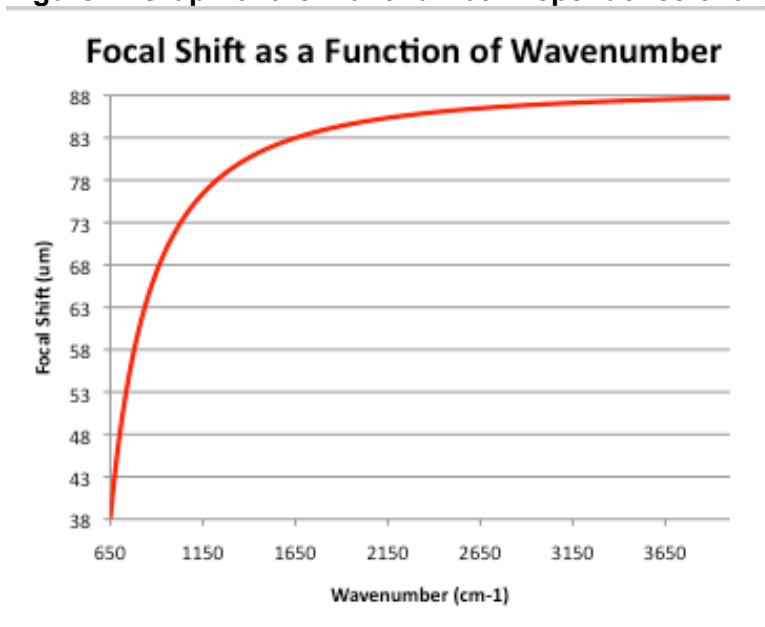
The focal shift was calculated using geometry, trigonometry, and Snell's Law ( $n_1 \sin \theta_1 = n_2 \sin \theta_2$ ). In addition, the dispersion of infrared and visible radiation causes the focal shift to be wavenumber (or wavelength) dependent, as shown in the following equation:

$$Focal\ Shift = t \times \left[ \left( \frac{\tan \Theta_{IR} - \tan \left( \frac{\sin^{-1} (n_{\lambda,air} \times \sin \Theta_{IR})}{n_{\lambda,IR}} \right)}{\tan \Theta_{IR}} \right) - \left( \frac{\tan \Theta_{Vis} - \tan \left( \frac{\sin^{-1} (n_{\lambda,air} \times \sin \Theta_{Vis})}{n_{\lambda,Vis}} \right)}{\tan \Theta_{Vis}} \right) \right] \quad (5)$$

where t is the thickness of the barium fluoride,  $\theta_{IR}$  and  $\theta_{Vis}$  are the angle of incidence for the infrared and visible light rays, respectively, and  $n_{\lambda,air}$ ,  $n_{\lambda,IR}$ , are the  $n_{\lambda,Vis}$ , are the associated wavelength-dependent refractive indices. The numerical aperture (NA) of the visible light lens in the ARO is 0.22, corresponding to a  $\theta_{Vis} = 12.7^\circ$ . The NA of the

infrared radiation of the ARO is 0.88, corresponding to a  $\theta = 61.6^\circ$ . However, because the infrared radiation does not pass through the central visible light optics, the average incident angle of infrared radiation,  $\theta_{IR}$ , is  $52.8^\circ$ . Figure 4 shows a graph of the calculated focal shift as it changes with wavenumber. The focal shift was calculated to be an average of 82  $\mu\text{m}$ , with a focal shift of 88  $\mu\text{m}$  for  $4000\text{ cm}^{-1}$  (2.5  $\mu\text{m}$ ) and 38  $\mu\text{m}$  for  $650\text{ cm}^{-1}$  (15.4  $\mu\text{m}$ ).

**Figure 4: Graph of the Wavenumber Dependence of the Focal Shift**



There was a small difference in the measured and calculated values for the focal shift, which may be due to the wavelength dependence of the calculated focal shift, or even slight variations in the thickness of the barium fluoride cover slip.

### Sample Preparation

For each sample, a few grains were transferred to the sample area of an infrared-reflective slide of the sealed-cell kit and rolled to flatness using a stainless steel roller. A 0.5-mm barium fluoride cover slip was placed on top of the double-sided adhesive tab to seal the preparation. A background was collected in infrared focus from an area under the cover slip with no sample present. Infrared focus was defined as the stage position along the z-axis where maximum interferogram signal was achieved. The slide was then repositioned in the x-y plane so that an infrared spectrum could be collected from the sample while in infrared focus. The resulting spectrum was processed using Thermo GRAMS/AI software to eliminate the carbon dioxide peak ( $2400 - 2300\text{ cm}^{-1}$ ) and compared against the library to determine HQI values using both the correlation and first derivative search algorithms within the Spectral ID software of the Thermo GRAMS Suite.

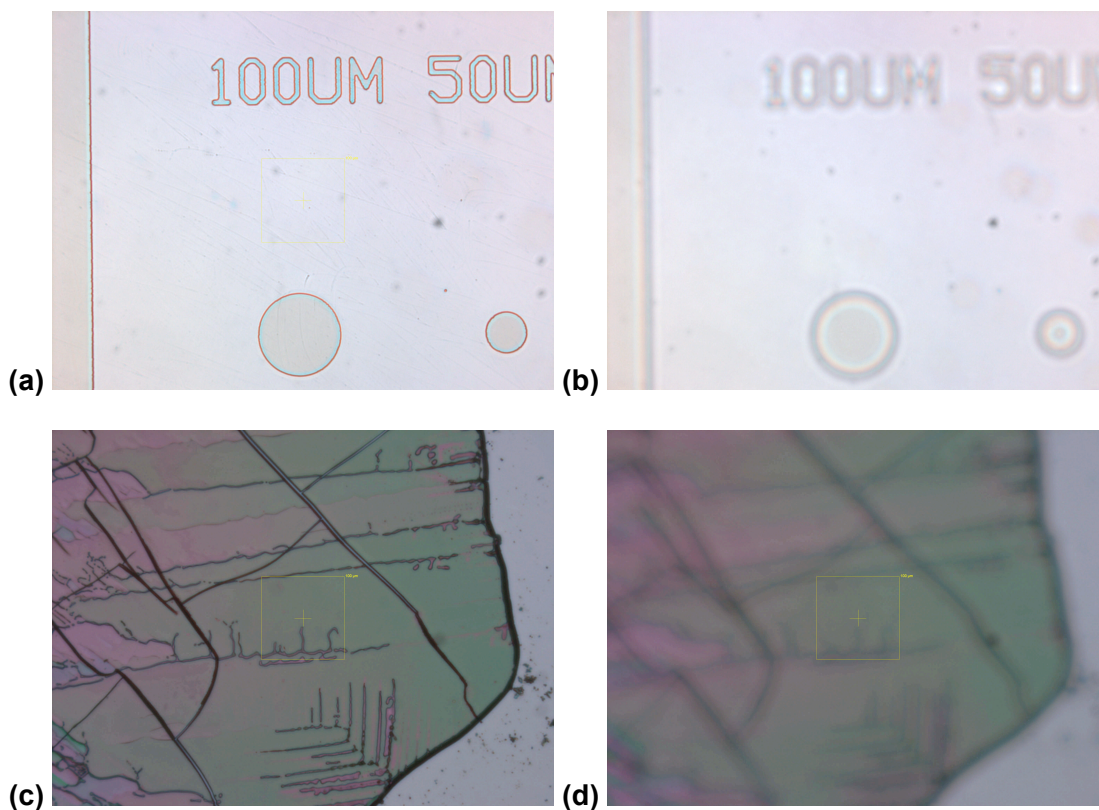
The same preparation was analyzed a second time from the same locations for both the background and the sample, but rather than optimizing to infrared focus, optimization for both the background and the sample were done using visible focus. Visible focus was defined as the stage position along the z-axis where the optimum visual image was achieved. Visible focus was approximately 90 micrometers from

infrared focus along the z axis when using the sealed cell's 0.5-mm barium fluoride cover slip.

This entire procedure as described within this "Sample Preparation" section was repeated a second time. Ultimately, two spectra were collected from each type of sample in infrared focus and two spectra were collected from each type of sample in visible focus.

To demonstrate the impact on visual quality when switching between visible and infrared focus, Figures 5 (a) and (b) shows a photoresist slide imaged through a barium fluoride cover slip. Photoresist was chosen for this demonstration because it is layered very thinly onto the slide and, therefore, can be focused very sharply. Figures 5 (c) and (d) show a sample of caffeine prepared for analysis in reflection-absorption mode, viewed through a barium fluoride cover slip. The images on the left show the slides in visible focus through the barium fluoride; the images on the right show the slides in infrared focus through the barium fluoride.

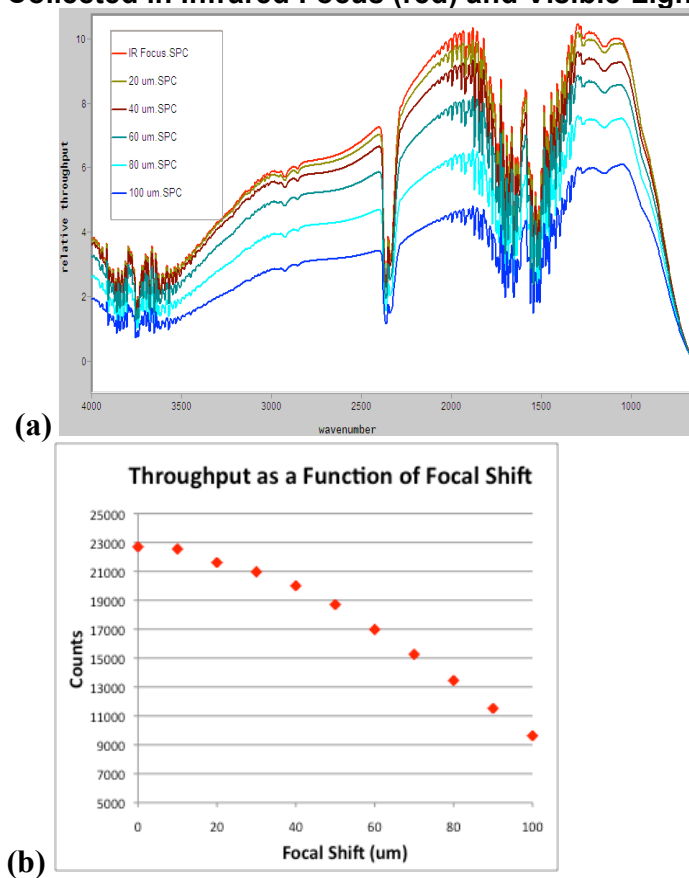
**Figure 5. Photomicrographs of a Photoresist Slide with a 0.5-mm Barium Fluoride Cover Slip in Visible Focus (a) and IR Focus (b), and a Caffeine Sample Prepared For Analysis in Reflection-Absorption Mode, with a 0.5-mm Barium Fluoride Cover Slip in Visible Focus (c) and Infrared Focus (d)**

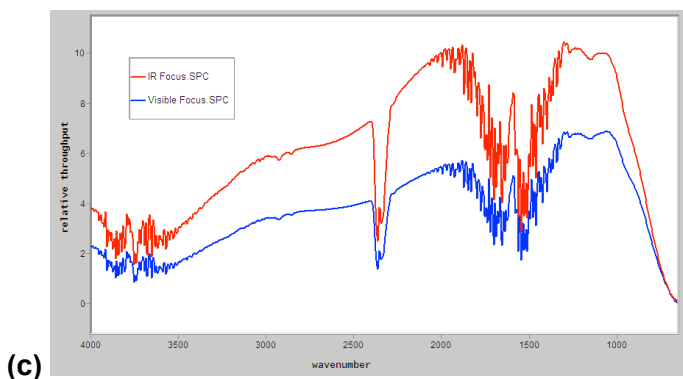


## Data and Results

Similar to the degradation of the visible image quality observed when a photomicrograph is captured when the microspectrophotometer is optimized for infrared focus, the throughput of the infrared signal decreases when the microspectrophotometer is optimized for visible focus. When the throughput of the infrared radiation is higher, better spectral quality will likely be achieved. Therefore, a decrease in the throughput will impact spectral quality. This decrease in throughput can be seen both on the intensity of the signal across the background infrared spectrum, and in the decrease in interferogram counts (Figure 6). The Figure 6 (a) shows throughput differences in infrared signal intensity across the spectrum; Figure 6 (b) shows throughput differences measured in interferogram intensity as a function of distance from the plane of infrared focus (focal shift). Decrease in infrared throughput is the result of the dispersion of infrared and visible light in barium fluoride. The visible and infrared focuses are not parfocal because barium fluoride disperses these signals, resulting in lower throughput when visible-light focus is employed during an infrared measurement. This is shown in Figure 6 (c), which displays the infrared signal intensity across the infrared spectrum for both visible and infrared focus.

**Figure 6. Infrared Signal Intensity Differences Across the Infrared Spectrum with Different Focal Shifts, (a) Graph of the Throughput as a Function of Focal Shift (b), and Infrared Signal Intensity Difference Across the Infrared Spectrum When Collected in Infrared Focus (red) and Visible-Light Focus (blue) (c).**





A consequence of decreased throughput is the increase in the measured root-mean-square noise of the infrared spectrum. Table 2 shows the calculated root-mean-square noise values for infrared spectra collected using various aperture sizes (100- $\mu\text{m}$ , 50- $\mu\text{m}$ , and 25- $\mu\text{m}$  squares) when no barium fluoride window is used, as well as when spectra are collected through a barium fluoride window in visible focus and infrared focus. It can be seen that when visible focus is used to collect an infrared measurement, the root-mean-square noise is significantly higher than when no barium fluoride is used, or when barium fluoride is used but the measurement is collected using infrared focus. When spectra are collected using smaller apertures, this increase in root-mean-square noise becomes even more significant. It is well known that smaller apertures will result in greater amounts of noise, but the effect of collecting the infrared spectra in non-optimal visible focus has considerable deleterious effects on the spectra, as demonstrated by an increase in the root mean square noise.

**Table 2: Calculated root-mean-square noise of spectra when collected in Visible Focus, Infrared Focus and with No Barium Fluoride when using a 100- $\mu\text{m}$  x 100- $\mu\text{m}$  aperture (a), 50- $\mu\text{m}$  x 50- $\mu\text{m}$  aperture (b), and 25- $\mu\text{m}$  x 25- $\mu\text{m}$  aperture (c).**

	No Barium Fluoride	IR Focus	Visible Focus
<b>100 <math>\mu\text{m}</math> aperture</b>	6.3E-05	7.1E-05	1.2E-04
<b>50 <math>\mu\text{m}</math> aperture</b>	1.3E-04	1.6E-04	3.1E-04
<b>25 <math>\mu\text{m}</math> aperture</b>	4.4E-04	5.9E-04	1.2E-03

Aside from observed differences in spectral quality, HQI of results were also different depending upon whether infrared or visible focus was employed to collect the spectrum. Results show that when using a correlation algorithm search, there was an average increase of 17% in HQI for spectra collected in infrared focus over those collected in visible focus. When using a first derivative correlation algorithm search, there was an average increase of 30% in HQI for spectra collected in infrared focus over those collected in visible focus. Thus, when analyzing through a barium fluoride cover slip, it is best to analyze the sample in infrared focus regardless of which search algorithm is used.

Tables 2 and 3 display the HQI results of the infrared library search analysis for four of the fifteen samples using the correlation algorithm (Table 3) and the first derivative correlation algorithm (Table 4). The HQI difference was calculated by subtracting the HQI for infrared focus from that for visible focus. The percent HQI was calculated by dividing the HQI difference by the HQI for infrared focus, and multiplying by 100.

**Table 3. HQI Results of the Infrared Library Search Analysis Using the Correlation Algorithm**

	HQI - correlation algorithm	HQI difference	Percent HQI difference
Chalk in infrared focus	0.175	0.058	33.1%
Chalk in visible focus	0.233		
Dipel in infrared focus	0.148	0.025	16.9%
Dipel in visible focus	0.173		
Flour in infrared focus	0.143	0.122	85.3%
Flour in visible focus	0.265		
Non-Dairy Creamer in infrared focus	0.101	0.041	40.6%
Non-Dairy Creamer in visible focus	0.142		

**Table 4. HQI Results of the Infrared Library Search Analysis Using the First Derivative Correlation Algorithm**

	HQI - 1st derivative correlation algorithm	HQI difference	Percent HQI difference
Chalk in infrared focus	0.197	0.057	28.9%
Chalk in visible focus	0.254		
Dipel in infrared focus	0.295	0.144	48.8%
Dipel in visible focus	0.439		
Flour in infrared focus	0.378	0.144	38.1%
Flour in visible focus	0.522		
Non-Dairy Creamer in infrared focus	0.397	0.211	53.1%
Non-Dairy Creamer in visible focus	0.608		

**Discussion:** When performing microspectroscopical analysis using a sealed cell, optimization of the infrared signal improves the quality of spectra collected. This improvement in spectral quality results in an improvement in the accuracy of the identification made when a spectrum is searched against electronic libraries of spectra. Searching of electronic databases of spectra is an important capability that can significantly decrease the amount of time it takes the analyst to identify the substance. In fact, if an accurate match against an electronic library is not achieved, it's possible the analyst may not be able to identify the substance without employing further test methods.

The use of barium fluoride in infrared systems is not unique to the sealed cell. Barium fluoride continues to be used extensively as a sample substrate in infrared instruments with slower optics. The near-normal incidence of radiation in these systems



minimizes the dispersion observed. However, infrared microscopes require fast optics with higher numerical apertures. As a consequence, the higher angles of incidence increase the effects of dispersion on the bending of radiation. While this dispersion is typically within a reasonable workable range for slow optics, it can be a problem for infrared microscopes with fast optics. In these instances, control of experimental procedures can minimize the effects of dispersion on the infrared spectrum.

When using a sealed cell with a barium fluoride cover slip, achievement of optimal infrared signal is performed differently depending upon the type of infrared measurement performed. When a reflection-absorption measurement is performed, optimization of the infrared signal is quite simple to achieve. During this type of analysis, incident radiation is focused onto the surface of an infrared reflective slide, reflects from this surface, and travels back through the microscope objective to the detector. As previously mentioned, the visible and infrared radiation are parfocal when the analysis is performed in air. Barium fluoride used in the sealed cell, however, disperses these beams differently and they are no longer parfocal when the sealed cell is used. Focus for either visible or infrared focus is achieved simply by adjusting the stage of the microscope along the z-axis, i.e., the stage is simply lowered or raised to optimize analysis. The analysis performed as part of this experiment indicates that optimization of infrared signal is important and should be performed for the best possible spectral quality and results.

## References

- (1) M. Polyanskiy, "Refractive Index Database: Optical Constants of BaF<sub>2</sub> (Barium Fluoride)". 2016. <http://refractiveindex.info/?shelf=main&book=BaF2&page=Li> [accessed Mar 07, 2016].
- (2) G.L. Carr. "Resolution Limits for Infrared Microspectroscopy Explored with Synchrotron Radiation". *Rev. Sci. Instrum.* 2001. 72(3): 1613-1619.
- (3) D.L. Wetzel. "A New Approach to the Problem of Dispersive Windows in Infrared Microspectroscopy". *Vib. Spectrosc.* 2002. 29: 291-297.
- (4) K.L.A. Chan, S.G. Kazarian. "Correcting the Effect of Refraction and Dispersion of Light in FT-IR Spectroscopic Imaging in Transmission through Thick Infrared Windows". *Anal. Chem.* 2013, 85: 1029-1036.
- (5) K.L.A. Chan, S.G. Kazarian. "Aberration-free FTIR spectroscopic imaging of live cells in microfluidic devices". *Analyst.* 2013. 138: 4040-4047.
- (6) GRAMS/AI Help Resource. [Computer Software]. Thermo Scientific.
- (7) C. Poore, P.A. Emanuel. "Screening Tools for Suspicious Powders: Do They Work?". *Evid. Tech. Mag.* September-October 2009: 10-13.